This manuscript has been published as:
Julian Rechmann, Maciej Krzywiecki, Andreas Erbe: Carbon-sulfur bond cleavage during adsorption of octadecane thiol to copper in ethanol. *Langmuir*, **35**, 6888-6897 (**2019**). DOI: 10.1021/acs.langmuir.9b00686

Final published version of the manuscript is available from:
https://doi.org/10.1021/acs.langmuir.9b00686

Carbon-sulfur bond cleavage during adsorption of octadecane thiol to copper in ethanol

Julian Rechmann,[†] Maciej Krzywiecki,[‡] and Andreas Erbe[*,¶,†]

†*Max-Planck-Institut für Eisenforschung GmbH, Max-Planck-Str. 1, 40237 Düsseldorf, Germany*

‡*Institute of Physics - CSE, Silesian University of Technology, Konarskiego 22B, 44-100 Gliwice, Poland*

¶*Department of Materials Science and Engineering, NTNU, Norwegian University of Science and Technology, 7491 Trondheim, Norway*

E-mail: ODT-on-Cu@the-passivists.org

Phone: +47 73594048

Abstract

The effect of the solvent on the formation of thiol self-assembled monolayers (SAMs) on oxide-covered, reactive metals is more involved than in the well-studied gold-thiol system. In this work, copper covered with a native oxide was modified with 1-octadecanethiol (ODT) in either tetrahydrofuran (THF) or ethanol. Infrared (IR) spectroscopy indicated the formation of crystalline chain packing of alkyl chains from both solvents. Surface coverage was approximately equal in both systems, with differences in tilt angles of the chains. A detailed analysis by X-ray photoelectron spectroscopy (XPS) showed the formation of Cu_2S and copper-bound carbon when the adsorption was carried out in ethanol. This observation can be explained by the cleavage of the

C-S bond in ODT during adsorption. Based on the analogy of preparations, we reason that the solvation of ODT in ethanol must be such that it weakens the C-S bond in ODT, thus enabling the cleavage of this bond. Based on the evidence presented here, it is not possible to distinguish between surface solvation and bulk solvation. Electrochemical linear sweep voltammetry show that SAMs from both solvents have an enhancing protective effect compared to the native oxide layer. The results from this work show interesting possibilities for the preparation of adsorbed monolayers with chemical interaction to reactive metals, with some similarities to carbene-based SAMs.

Introduction

Since late 1980s, much effort has been put into investigating self-assembled monolayers (SAMs).[1,2] Different techniques for SAM deposition have been developed, structure and electronic coupling to the substrate has been analyzed, but also evaluation of the resistance against degradation, thermal and physical stresses.[3] Especially for electronic devices, it is important to prepare robust and long-living materials with desired properties. In particular, detailed knowledge of the interfacial chemistry is crucial for achieving stable systems. Widely used and most studied systems are thioles on gold.[1,4] Their chemistry and formation kinetics have been well investigated. In particular, numerous studies for thiols and related systems on gold have shown that the choice of solvent affects the obtained molecular arrangement, such as domain sizes or order, or composition of mixed SAMs.[5–11]

For oxide-covered metals, the surface chemistry is more involved, as is the effect of the solvent on the deposition. For example, thiols can reduce the native oxide on nickel, the reduction depends on the solvent, and has consequences for the resulting SAM structure.[12] Of great interest is also copper, e.g., in copper-based electrical contacts; copper is relatively cheap and has a high electric conductivity.[3] Thiole SAMs have, e.g., been explored for corrosion protection during wire bonding of copper structures.[13] The complex interactions between solvents and native oxide, as well as possible oxidation reactions during surface

modification under ambient conditions, may, however, be problematic on copper.[14–18]

The self-assembly of thiols on copper covered with a native oxide was subject to several investigations, focusing on the interfacial chemistry and its conditions while chemisorption takes place.[14–16,18,19] In case of freshly evaporated Cu, cuprous oxide Cu_2O is the predominantly found oxide.[20] As a first step of the adsorption mechanism, thiols reduce the oxide layer under formation of disulfides,[14,21–23]

$$2\,CH_3(CH_2)_nSH + CuO \longrightarrow (CH_3(CH_2)_nS)_2 + Cu + H_2O, \tag{1}$$

or

$$2\,CH_3(CH_2)_nSH + Cu_2O \longrightarrow (CH_3(CH_2)_nS)_2 + 2Cu + H_2O. \tag{2}$$

Afterwards, self-assembly of the organic molecules takes place on the reduced surface according to[15]

$$2\,CH_3(CH_2)_nSH + Cu \longrightarrow CH_3(CH_2)_nS{-}Cu + \frac{1}{2}\,H_2, \tag{3}$$

or an analogous reaction with the disulfide. A combination of steps (1) and (2) with step (3) may be possible. Formally, the reaction can be treated as an oxidative addition of the S-H bond to the copper surface with reductive elimination of the mercaptan hydrogen atom. Despite initial reduction of oxide, copper reoxidises at ambient conditions, though the SAMs slow down reoxidation compared to reduced surfaces without SAMs.[24–27]

Copper may react with certain solvents, such as alcohols. Ethanol has previously been found to lead to SAMs with lower order on copper.[19,21] Ethanol may react itself with the copper surface, with consequences for SAM formation.[18] In general, solvent polarity has an effect on the reduction of the native oxide, and the barrier properties of the resulting SAM.[16]

In the present work, copper evaporated on Si(100) by physical vapour deposition (PVD) was modified with 1-octadecanethiol (ODT) in tetrahydrofuran (THF) and ethanol. Infrared (IR) spectrocopy and X-ray photoelectron spectroscopy (XPS) were used to study the structures of the thin films. Time dependent water contact angle experiments were performed, as

well as linear sweep voltammetry (LSV) measurements in sodium hydroxide, in order to compare the stability of the obtained SAM-covered surfaces. The main focus of this manuscript is the comparison of the SAMs obtained in THF with those obtained in ethanol, and an elucidation of the effect ethanol has on SAM formation. Within this work, the term "SAM" will be used in the wider sense, including systems which may not be strictly monolayers, but only few nm thick, and systems which may adsorb not only in solution. Furthermore, the heterogeniety of the system has not been systematically investigated.

Experimental Section

Materials

Silicon wafers (diameter 4 inch, thickness 0.5 mm) were obtained from Siegert Wafer (Aachen, Germany). 1-Octadecanethiol, sodium hydroxide pellets, absolute ethanol and THF were sourced from VWR. All chemicals were used as received.

Substrate preparation

Prior to physical vapour deposition (PVD), silicon wafers were carefully cleaned in a solution of Tickopur TR3 (Dr. H. Stamm, Berlin, Germany), then washed with an excess of deionized water and dried under a stream of nitrogen. The silicon wafers were subsequently coated with 10 nm of chromium and 200 nm of copper at a deposition rate of 2 Å$\cdot$ s^{-1}, monitored by a quartz crystal oscillator (Leybold Inficon), assuring a smooth and uniform surface. Copper evaporated under similar conditions as here has been shown to be strongly {111} textured.[28] The copper substrates were stored in a desiccator until adsorption experiments were executed.

Surface modification of oxide-covered copper

Copper substrates were cleaned with acetone and immersed in 5 mL of a freshly prepared 0.1 mM solution of ODT in THF. In case of modifying samples with ODT in ethanol, a saturated solution was used. (Preparation of a 0.1 mM solution left undissolved ODT). The substrates were left in the solution for 3 h. Afterwards, samples were taken out of the solution and rinsed with an excess of both ethanol and THF. Finally, substrates were dried with a stream of nitrogen and stored under vacuum until further analysis.

Surface characterization methods

Infrared (IR) spectroscopy. IR spectra were taken with a Bruker Vertex 70v Fourier transform IR spectrometer, operated under vacuum. The absorption spectra were recorded with a spectral resolution of 4 cm^{-1} using p-polarized light at an angle of incidence of 80°. The spectrometer was equipped with a middle band mercury cadmium telluride detector which was cooled with liquid nitrogen 1 h before the measurements. Prior to surface modification, background spectra were obtained from freshly cleaned copper samples. The absorbance spectra shown in this work were recorded against these backgrounds. The absorbance A is defined as $A = -\log_{10} \frac{I_{\text{sample}}}{I_{\text{background}}}$, where I is the wavenumber-dependent intensity recorded at the detector. Each sample was measured with 1000 scans.

Tilt angles of the alkyl chains have been estimated by using the integrated absorbance of the asymmetric stretching mode of terminal CH_3 at 2954 cm^{-1} and the antisymmetric CH_2 stretching mode at 2917 cm^{-1}. These modes have a transition dipole moment parallel and perpendicular to the C-C-C plane, respectively.[29] The tilt angle γ of the surface normal of the methylene group's H-C-H planes was thus determined as[30]

$$\langle \cos^2 \gamma \rangle = \frac{D^{(\text{refl})}}{D^{(\text{refl})} + 2D^{(\text{trans})}}, \tag{4}$$

where $D^{(\text{refl})} = A(CH_3)/A(CH_2)$ is the ratio of the absorbances of the aforementioned asym-

metric CH_3 stretching mode and the antisymmetric CH_2 stretching mode, respectively, in a reflection experiment. $D^{(\mathrm{trans})}$ is the respective ratio from an experiment in transmission geometry of a randomly oriented sample.

X-ray photoelectron spectroscopy (XPS). XPS was performed to investigate the chemical composition of the sample surfaces (Quantera II, Physical Electronics) applying a monochromatic Al Kα X-ray source (1486.6 eV) operated at a pass energy of 55 eV and a step size of 0.05 eV. The takeoff angle $\theta = 45°$, defined here as angle between analyzer axis and surface normal. The binding energy scale was referenced to the C-C signal at 284.8 eV.[31] The quantitative analysis was carried out with CasaXPS software. Spin orbit splitting was used in peak fitting as implemented in standard procedures in the software. In this work, only the commonly discussed components will be treated. For interpretation, commonly used online databases were used as starting points (`http://xpssimplified.com/elements`; `https://srdata.nist.gov/xps/Default.aspx`).

The surface coverage Γ of different sulfur species on copper was determined from comparing the peak intensities of the respective component of the S 2p to the Cu $2p_{3/2}$ peak of the substrate as[32]

$$\Gamma(\mathrm{S}) = \frac{A_\mathrm{S}}{A_\mathrm{Cu}} \frac{S_\mathrm{Cu}}{S_\mathrm{S}} \rho(\mathrm{Cu}) \lambda(\mathrm{Cu}) \sin(\theta) \frac{\mathrm{e}^{d/[\lambda(\mathrm{S;org}) \sin(\theta)]}}{\mathrm{e}^{d/[\lambda(\mathrm{Cu;org}) \sin(\theta)]}}. \tag{5}$$

The area ratio of the respective S 2p component and Cu $2p_{3/2}$ is denoted as $\frac{A_\mathrm{S}}{A_\mathrm{Cu}}$, while $\frac{S_\mathrm{Cu}}{S_\mathrm{S}}$ represents the ratio of the respective atomic sensitivity factors. In eq. (5), $\rho(\mathrm{Cu}) \approx 0.14 \cdot 10^{22}$ atoms/cm^3 is the number of copper atoms per unit volume in the surface oxide,[33] $\lambda(\mathrm{Cu}) \approx 0.78$ nm is the inelastic mean free path (IMFP) of Cu photoelectrons in the substrate,[33,34] $\lambda(\mathrm{S;org})$ and $\lambda(\mathrm{Cu;org})$ are the IMPFs of the respective photoelectrons in the organic layer, and d represents the thickness of the SAM. For sulfur and copper photoelec-

trons, the IMFP $\lambda(X;\mathrm{org})$ in the organic layer was obtained as[32]

$$\lambda = 9.0\ \text{Å} + 0.022\ \text{Å}(\text{eV})^{-1} E_{\text{kin}}, \tag{6}$$

with the measured photoelectron kinetic energy E_{kin}. Thus, IMFPs of S 2p and Cu $2p_{3/2}$ in the organic monolayers are $\lambda(\mathrm{S};\mathrm{org}) \approx 3.81$ nm and $\lambda(\mathrm{Cu};\mathrm{org}) \approx 2.12$ nm.

Contact angle. Water contact angle measurements were carried out with ultra pure water using an OCA 30 goniometer (Dataphysics) at ambient temperature. Contact angle data were determined by the sessile drop method; the drop volume was fixed to 5 µL. The last contact angle corresponds to the last possible measurement before the water droplet evaporated completely. Angles exhibited an accuracy of $\approx 5°$, determined from repeated measurements.

Electrochemical experiments

Electrolytes. Potentiodynamic measurements were carried out in a 0.1 M sodium hydroxide solution (pH = 13.2) and in borate buffer solution (0.075 mol $Na_2B_4O_7 \cdot 10\ H_2O$, 0.3 mol H_3BO_4 in 1 L double deionised water; pH = 8.6). For preparation, ultrapure water (PureLab Plus system, Elga, 18.2 MΩ cm^{-1}) was used.

Linear sweep voltammetry (LSV). Linear polarization experiments were executed in a home-made three electrode setup using an Ivium CompactStat potentiostat. The measured specimens had an area of 0.785 cm^2. As counter electrode, a graphite rod was used. A saturated Ag|AgCl|3M KCl electrode (Metrohm, Filderstadt, Germany) served as reference electrode (equilibrium potential E^0 = +210 mV with respect to standard hydrogen electrode).[35] Copper with its native oxide, and copper modified with ODT in THF and ethanol, respectively, were used as working electrodes. All measurements were done at a scan rate of 1 mV/s with a step size of 1 mV.

Evaluation of electrochemical data with the Stern-Geary equation. The corrosion parameters shown in this section were obtained by applying Stern-Geary analysis to different data. Polarization resistance R_{P} was determined as the slope of the linear polarization curve from -10 mV to $+10$ mV around the corrosion potential E_{corr}. Anodic and cathodic Tafel slopes b_{a} and b_{c}, respectively, were obtained from linear regions of the Tafel plot. As many graphs do not show perfect Tafel behavior, the branch (anodic or cathodic) which exhibited closest to linear behaviour was fitted first. The second branch was fitted in a way that the potential value of the crossing point equals E_{corr}. Corrosion current densities i_{corr} were then calculated according to[36]

$$i_{\mathrm{corr}} = \frac{b_{\mathrm{a}} \cdot b_{\mathrm{c}}}{R_{\mathrm{P}} \cdot \ln(10) \cdot (b_{\mathrm{a}} + b_{\mathrm{c}})}. \tag{7}$$

Typically, five samples were analyzed for each system. Uncertainty estimates of electrochemical parameters are presented as standard deviations from the different samples.

Results and discussion

Macroscopic surface properties and stability

Copper samples which were left for 3 h in THF showed whitish patterns on the surface. Samples in ethanol did not show any optical differences on the surface. Contact angle measurements were executed for bare copper and oxide-covered copper modified in each solvent (Fig. 1). Non-modified copper exhibited an initial contact angle of $(102 \pm 3)^\circ$. The contact angle decreased constantly until the water droplet completely wetted the metal substrate after 20 min. In comparison, the water droplet on the modified surfaces exhibited initial contact angles of $(114\pm2)^\circ$ and $(131\pm2)^\circ$ for the ODT/THF and ODT/ethanol system, respectively, showing increased hydrophobicity. Interestingly, the water droplet evaporated on samples modified in THF after 30 min with a last measurable contact angle of $(84 \pm 2)^\circ$. In case of samples modified in ethanol, the water evaporated after 33 min, with a much lower

contact angle of $(31 \pm 4)°$.

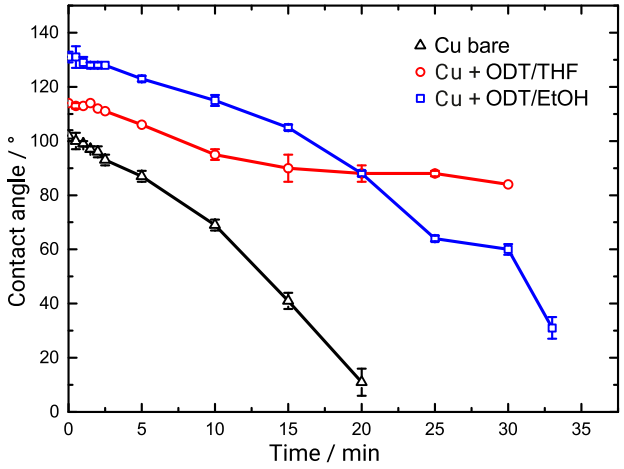

Figure 1: Contact angles of bare copper (—) and copper modified with ODT in THF (—) and ethanol (—), respectively, as a function of time.

The differences in water contact angle inspired electrochemical linear polarisation experiments to evaluate the electrochemical properties of the SAMs compared to the native oxide of copper. Recorded voltammograms in NaOH are shown in Fig. 2 and calculated parameters in NaOH and borate buffer are summarized in Table 1. The corrosion potential E_{corr} of bare copper and the sample modified in THF in NaOH is around 0 V. The E_{corr} of the sample functionalized in ethanol is shifted 50 mV negatively. Comparing i_{corr} in NaOH of the systems, oxide-covered copper dissolved by a factor of 250 faster than samples modified in THF, which, on the other hand, dissolve about 25 times faster than those functionalized in ethanol.

Table 1: Electrochemical parameters of oxide-covered copper modified with ODT in either ethanol or THF. LSV was executed in ambient atmosphere in 0.1 M NaOH (pH = 13.2) and in borate buffer solution (pH = 8.6)

System	$E_{\mathrm{corr}}^{(\mathrm{NaOH})}$ mV	$R_{\mathrm{P}}^{(\mathrm{NaOH})}$ $\Omega \cdot \mathrm{cm}^2$	$i_{\mathrm{corr}}^{(\mathrm{NaOH})}$ $\mathrm{A} \cdot \mathrm{cm}^{-2}$	$E_{\mathrm{corr}}^{(\mathrm{Borate})}$ mV	$R_{\mathrm{P}}^{(\mathrm{Borate})}$ $\Omega \cdot \mathrm{cm}^2$	$i_{\mathrm{corr}}^{(\mathrm{Borate})}$ $\mathrm{A} \cdot \mathrm{cm}^{-2}$
Bare Cu	-7	$1.6(1) \cdot 10^3$	$8.1(2) \cdot 10^{-6}$	181	$1.25(5) \cdot 10^4$	$1.04(3) \cdot 10^{-6}$
ODT/THF	-1	$3(1) \cdot 10^4$	$3(1) \cdot 10^{-7}$	155	$5.5(7) \cdot 10^6$	$4.4(7) \cdot 10^{-9}$
ODT/ethanol	-51	$6.9(9) \cdot 10^6$	$1.3(1) \cdot 10^{-9}$	132	$1.10(3) \cdot 10^8$	$2.0(2) \cdot 10^{-10}$

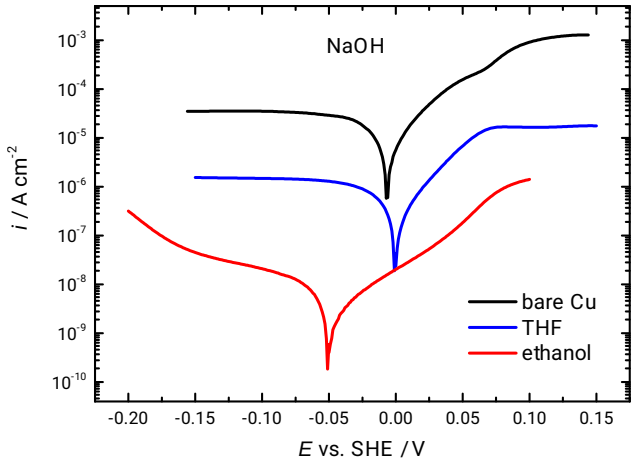

Figure 2: Tafel plots of oxide-covered copper (—) and modified with ODT in either THF (—) or ethanol (—). Measurements were executed in ambient atmosphere and in 0.1 M NaOH (pH = 13.2).

The cathodic branches of the voltammograms for bare Cu and samples modified in THF showed the typical potential-independent current observed for a diffusion limited process, which is typically assigned to the oxygen reduction reaction (ORR). The ORR current was one and a half orders of magnitude lower on the sample modified in THF compared to pure copper. For the ethanol modified sample, a certain slope was observed, while the current was 2 orders of magnitude lower than for the same SAM prepared in THF.

On the anodic side in NaOH, there was an inflection point around +70 mV in all three Tafel plots. In case of bare copper, the formation of a passivation layer is indicated, but the anodic current density i_a kept rising till +134 mV.

Surface characterization

The differences in contact angle and electrochemical behaviour between the differently prepared SAMs indicate structural or compositional differences between the SAMs prepared in the different solvents, with the latter being not expected a priori. These differences were investigated by IR spectroscopy and XPS. After 3 h of incubation time, samples were first analyzed by IR spectroscopy. The recorded spectra are shown in Fig. 3. Positions of the

signals and their assignments are summarized in Table 2. In both spectra, the stretching modes of the aliphatic methyl and methylene groups are well resolved. The positions of the antisymmetric and symmetric CH_2 stretching modes, ≈2920 cm^{-1} and ≈2850 cm^{-1}, respectively, show that the alkyl chains are structured in an all-trans conformation.[37,38] An all-trans conformation of aliphatic chains is known to indicate well packed and crystalline organic structures.[6,39] The methylene bending vibrations are well visible in case of samples modified in ethanol at 1471 cm^{-1}. Peaks in samples of copper modified with ODT in THF have only 2/3 the absorbance of the samples from ethanol. The tilt angle between molecule's main axis and surface normal was evaluated by eq. (4) as 36° for samples form ethanol and 45° for samples from THF. The presence of typical alkyl chains signatures in the IR is a proof that adsorption to the surface took place, with largely intact alkyl chains.

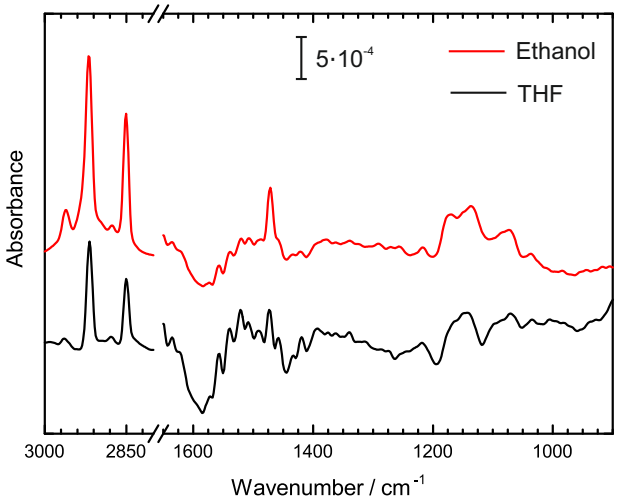

Figure 3: IR spectra of oxide-covered copper modified with ODT in either ethanol (—) or THF (—). Spectra have been vertically offset for clarity.

XPS gives the possibility to investigate the interfacial chemistry of the differently treated samples. The main interest lies in how the organic molecules are bound to the surface and what type of oxidized copper species are present. Spectra are shown in Fig. 4. Positions of the signals and their assignments are summarized in Table 3. For reference, spectra recorded on the pure substrate exposed to the respective solvent for the same time as for surface

Table 2: Characteristic IR peak positions and assignment to vibrational modes based on similar systems[6,29,37,38] of oxide-covered copper modified with ODT either in ethanol or THF

Origin	Assignment	Peak Position / cm^{-1}	
		THF	ethanol
CH_3	methyl C-H asym. stretch	2964	2962
CH_2	methylene C-H asym. stretch	2918	2920
CH_3	methyl C-H sym. stretch	2877	2875
CH_2	methylene C-H sym. stretch	2850	2850
CH_2	methylene C-H bend	1473	1471

modification are shown in Fig. 4a. These spectra are important for comparison, but their implications shall not be discussed in order to understand the nature of the adsorbed species after exposing copper with its native oxide to THF or ethanol. No survey spectra of any sample shows the presence of additional elements, e.g., from contaminations.

This discussion shall focus on the spectra of the modified copper (Fig. 4b) and shall proceed from the S 2p peak. Binding energies for thiolates bound to copper are well known from literature. Their S $2p_{3/2}$ peak is centred between 162.1 eV,[15,21] and 162.8 eV.[40–42] The S $2p_{3/2}$ peaks in this work are found at 162.2 eV and 162.6 eV, i.e. within the range reported in the literature for thiolates. In samples prepared from ethanol, there was a second sulfur species present at 160.9 eV (Fig. 4). This position is attributed to copper sulfides,[15,43–45] with sulfur in oxidation state -2. This sulfur species was at best present in traces in samples functionalized in THF, where only a shoulder at noise level was detected. (Differences in the peak positions for the main thiolate peak between the samples here and between this work and literature may result from the peak fitting associated with the low binding energy component, from the presence of different surfaces, and from differences in referencing). On both surfaces, amounts on the noise level of oxidized sulfur, with a peak centred around 168 eV, may also have been present. These amounts have not been considered in the fitting.

C 1s spectra for samples from THF and ethanol (Fig. 4b; Tab. 3) showed main signals at binding energies of 284.8 and 285.5/285.7 eV, which are assigned, respectively, to C-C/H bonds and to bonds of C with more electronegative atoms (labelled "C-O"). Interestingly,

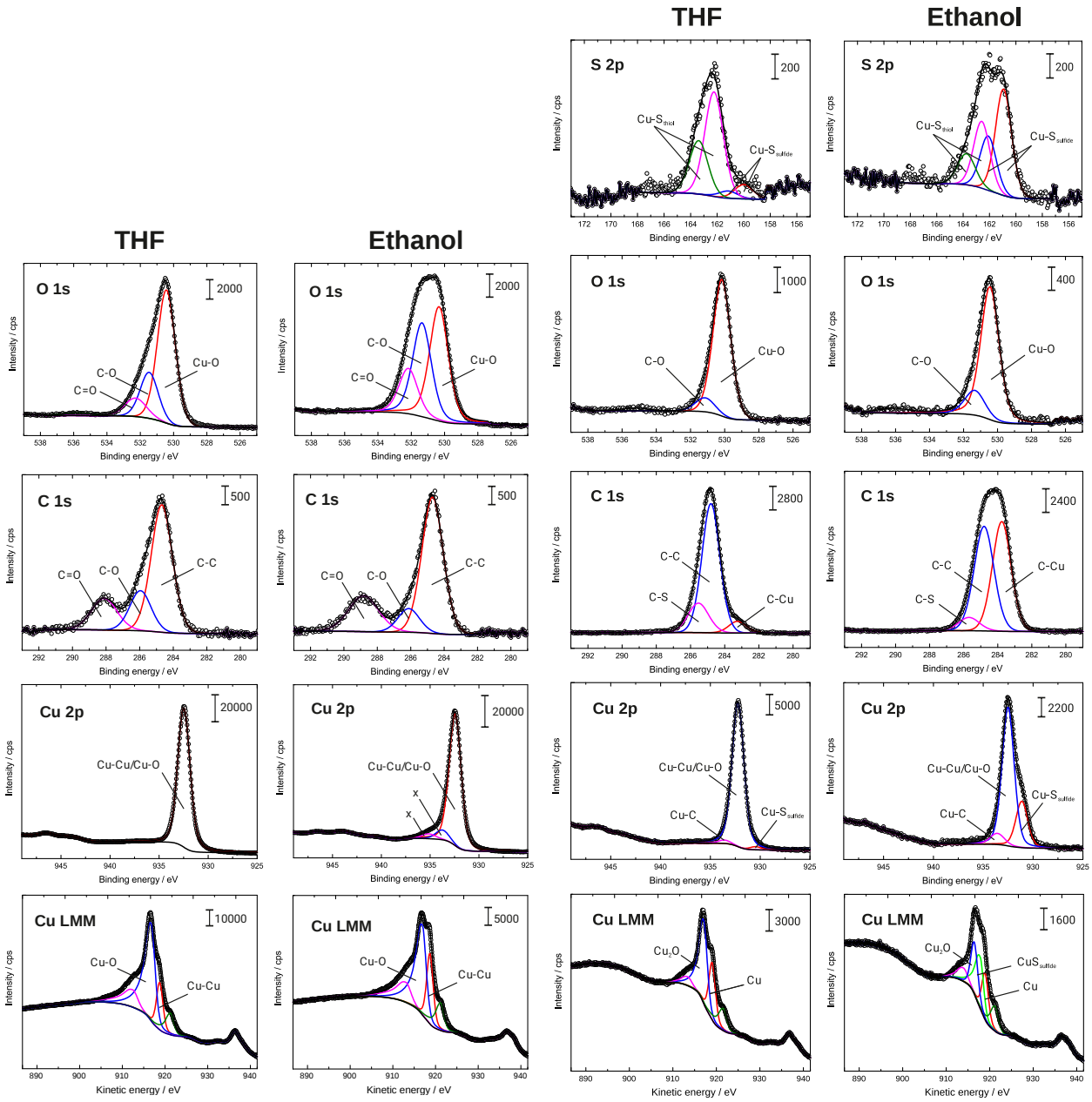

Figure 4: High resolution XP spectra in the S 2p, Cu LMM, Cu 2p, O 1s and C 1s regions of oxide-covered copper (a) exposed to THF and ethanol and (b) modified with ODT either in THF or ethanol. Note the different lengths of the scale bars.

there was a third compound observed for samples modified in THF and ethanol at 283.2 and 283.8 eV, respectively. In samples from ethanol, this component exhibited the same intensity as the signal from C-C bonds in the spectrum, with ≈47 % of the C 1s intensity. In THF

Table 3: Peak position (B.E. - binding energy in eV, K.E. - kinetic energy in eV), percentage of respective component and residual standard deviation (res. S.D.) from fitting of high resolution XP spectra (Fig. 4). Not all components have been included. C/S ratio of oxide-covered copper modified with ODT in either THF or ethanol. Only the components related to ODT molecules have been included in the calculation of the C/S ratio. Obtained ratios are compared with stoichiometric (stoich.) values based on composition

peak	component	THF			ethanol		
		B.E.	%	res. S.D.	B.E.	%	res. S.D.
S $2p_{3/2}$	Cu-S (sulfide)	160.0	12	0.913	160.9	61	0.951
	Cu-S (thiol)	162.2	88		162.6	39	
C 1s	C-Cu	283.2	7		283.8	47	
	C-C	284.8	74	1.839	284.8	47	1.379
	C-S	285.5	19		285.7	6	
O 1s	Cu-O	530.2	87	1.238	530.4	80	0.781
	C-O	531.1	10		531.3	16	
Cu $2p_{3/2}$	Cu-S (sulfide)	930.5	2		931.1	23	
	Cu/Cu_2O	932.2	96	2.172	932.5	70	1.500
	Cu-C	933.6	2		933.6	7	
		K.E.	%	res. S.D.	K.E.	%	res. S.D.
Cu LMM	Cu	919.0	26		919.0	21	
	CuS (sulfide)	-	-	2.822	917.8	31	2.067
	Cu_2O	917.1	52		916.5	24	
element ratio							
measured C_C/S_C		21.6			28.8		
stoich. C_C/S_C for ODT		18			18		

samples, this component only accounted for ≈7 % of the C 1s intensity. The observed signal in the C 1s spectrum at lower binding energies than aliphatic carbon indicates a chemical bond between carbon and a more electropositive element, which in this case can only be copper. The bond is comparable to the situation in metal carbides.[43] The intensity ratios of aliphatic carbon to carbide bound carbon were ≈1 in ethanol and ≈11 in THF. Because of the likely lateral heterogeneity of the surfaces, no further analysis of this ratio was conducted.

From S 2p and C 1s spectra, the C/S ratios were calculated with signals attributed to intact ODT only. The integral of the C 1s component attributed to C-C/H was used for

the C intensity, and the S 2p component attributed to S bound to C was used for S. The obtained ratios are 28.8 and 20.6 for samples modified in ethanol and THF, respectively. In case of samples from THF, SAMs were intact and the calculated value is in close agreement with the theoretical one of 18. In case of copper functionalized in ethanol, the value is higher than expected. In both cases, ratios may be altered by adventitious carbon, which may originate from adsorbed solvent or from atmospheric contaminations. The presence of the C-O-C component is a strong indication for the presence of such a component. In THF, the attenuation of the S 2p signal in the alkyl chain part of the SAMs also contributes to the deviations encountered.

The Cu 2p spectra of the differently prepared samples (Fig. 4b; Tab. 3) were fitted with three components for a consistent data interpretation. The main component is assigned to contain both metallic copper and Cu^{I}. The component at lower binding energies is consistent with signals from sulfur-bound copper, attributed to sulfide.[44] The intensity ratio of this component between ethanol and THF samples is 6.6, indicating a higher fraction of sulfide in ethanol than in THF. For the same system, the signal at higher binding energies originates either from CuO or Cu-C. Because of the very weak satellite peaks around 946.3 eV, Cu-C is the most probable recorded species.

Additional information about the chemical state of the species at the interface can be obtained from the Auger LMM peaks detected in the XP spectra (Fig. 4b; Tab. 3). For samples functionalized in THF, Cu LMM was fitted with four components. The dominating peaks are attributed to the existence of Cu^{0} (921.7 eV and 919.0 eV) and Cu_2O (kinetic energy 917.1 eV and 916.5 eV).[15,19] The peak at lower kinetic energies belongs to energy loss features (913.4 eV). This observation shows that Cu_2O is present only as layer of thickness of less than three times the attenuation length in the oxide layer of the electrons originating from the metal. Using a value of 0.83 nm as electron attenuation length in the dominating Cu_2O,[46,47] the layer thickness must be 1-1.5 nm with the signal observed. The same signals as in samples from THF can be observed for samples treated in ethanol. In these samples, however, an

additional component is present at 918.8 eV. Thus, the Cu LMM Auger transition was altered because of the presence of another compound. In line with the interpretation of the Cu 2p, this component must be related to the component detected at 931.1 eV Cu 2p binding energy, hence is assigned to Cu_2S. The energy value coincides with the measured position of copper sulfide layers on polyamide films.[48] Intuitively, one would expect the component to be on the opposite side of the metallic copper peak, based on its Cu 2p spectrum; the observation of the opposite shift is likely because of the different physics of the Auger and the photoelectron emission processes.[49] Cu LMM spectra overall support the interpretation of the components discussed previously.

O 1s spectra show two distinct signals at binding energies of 530.2 (530.4) eV and 531.1 (531.3) eV, on samples modified in THF (ethanol). These signals are attributed to Cu-O of Cu_2O and C-O bonds of adventitious carbon, respectively.[50] Observed intensities in the spectra are consistent with the interpretation that less Cu_2O is present on Cu samples modified with ODT in ethanol, as the respective intensity in the O 1s is only half the one from the samples in THF. The component at higher binding energies supports the interpretation of the presence of organic contamination from atmosphere or residual solvent on the sample surfaces.

Further information were obtained from surface coverage calculations on the basis of the S 2p signal [Eq. (5); Table 4], assuming an equivalent SAM thicknesses d of 1.29 nm. Only surface bound thiols of intact ODT molecules were used ($Cu - S_{thiol}$). For both differently treated samples, the surface coverage amounts to 4.0 ODT molecules/nm^2. A similar value of both systems is in line with IR experiments, since crystalline monolayers on both samples lead to closed packed molecules, and similar absorbance was observed. However, if the signal of the sulfide species is considered ($Cu - S_{sulfide}$), densities of 0.5 and 6.4 bonds/nm^2 were obtained for samples from THF and ethanol, respectively.

A repeat of IR measurements after XPS measurements showed no difference in the obtained spectra. Consequently, beam damage of the samples in XPS is negligible.

Table 4: Surface coverage of ODT and sulfide in the differently prepared samples calculated according to eq. (5)

System	ODT density molecules/nm^2	Cu-S density bonds/nm^2
ODT/THF	4.0	0.5
ODT/ethanol	4.0	6.4

Discussion of structural differences and their relation to electrochemical properties

The presence of sulfide in the S 2p spectra, the presence of Cu_2S in the Cu 2p and Cu LMM spectra, and the presence of carbide-like carbon in the C 1s spectrum all point to the fact that C-S bond cleavage occurs in ethanol, in form of a net reaction between copper and ODT of the type

$$3Cu + HS{-}(CH_2)_{17}CH_3 \longrightarrow Cu_2S + \frac{1}{2}H_2 + Cu{-}(CH_2)_{17}CH_3. \quad (8)$$

As also Cu-bound thiolate was observed in XPS, reaction (8) must occur in parallel to reactions (1)-(3). The comparison of the surface coverage of sulfidic sulfur with that of thiolate sulfur (Tab. 4) as well as of the C/S_{thiol} ratios for samples in THF and ethanol (Tab. 3) support this interpretation. Sulfide was not present in the original preparation, and the same ODT stock was used for the preparation of samples in both solvents. From the results obtained in this work, it is therefore safe to state that ODT reacts with Cu in ethanol other than by formation of a thiolate; instead, for a significant fraction of ODT molecules, the C-S bond breaks. While is known that organic ultra-thin layers, exhibiting sulfur moieties, are sensitive to X-ray irradiation,[51] the differences observed after preparation of SAMs with the same substance from THF and from ethanol indicate that differences must exist in the chemical bonds within those SAMs.

S-C cleavage was observed previously for 4-mercaptopyridine SAMs on Au(111) in ethanolic solution by in situ scanning tunelling microscopy and XPS.[52] Preparation of a complete

SAM proceeded within few minutes, successive degradation of the organic monolayer occured within hours, yielding sulfidised gold surfaces.[52] The most probable reason for the C-S cleavage observed here is a difference in the thiolate-metal bond strength. There is a competition between the metal-S and S-C bond of molecules covalently linked to the substrate.[53] The stronger the bond between metal and sulfur head atom, the weaker is the one between the sulfur and the carbon atom. This relationship has been worked out quantitatively and in detail in a series of articles comparing the situation for C-S and C-Se bonds for SAMs on Au(111) and Ag(111).[53–55] The S 2p peak position for the thiolate sulfur observed here shifted about 0.3 eV to more positive binding energies for samples modified in ethanol (Table 3) compared to those in THF. A positive shift indicates that more electron density is present between copper and sulfur instead being localized on the sulfur atom itself. As consequence, the S-C bond is weakened in ethanol, leading to S-C cleavage.[3] Considering the relative intensities of the thiolate-copper, more molecules are present on samples modified in THF compared to ethanol, which may be explained by dissolution of the forming alkane, because of C-S cleavage. We reason here that the different states of solvation of the ODT are responsible for the weakening of the C-S bond in this system.

Adsorption of ethanolates has been discussed for a similar system previously.[18] Also in other systems, solvent co-adsorption has been discussed as important mechanism steering the main monolayer formation.[56] The XPS reference data of pure copper exposed to the solvents does show certain adsorbed species. However, such adsorption occurs also in THF. A reasonable explanation for the fact that C-S cleavage is observed only in ethanol is that solvation of the thiol group in ethanol is such that the C-S bond weakens. This weakening may either occur in bulk, or via a coadsorption meachanism to the surface.

Comparing the intensities of the O 1s peaks related to Cu_2O between samples in THF and ethanol with and without ODT shows that the lowest oxide content is observed in ethanol in the presence of ODT. The oxide content is also reduced in THF, compared to the reference samples. Consequently, oxide reduction must have occurred in both systems, in line with

previous reports,[14–16,18,19,21] according to reactions (1)-(3). In the systems investigated here, oxide reduction was either not complete, or reoxidation was too fast, as previous reports did show surfaces on which the oxide was completely reduced.[14–16,18,19,21]

The fraction of carbide-like C observed in the C 1s peak is rather high, and suggests a further decomposition of the ODT molecules. However, IR spectra show the presence of significant amounts of intact ordered alkyl chains. So far, the high amount of carbide-like C remains to be difficult to understand. Local surface roughening may, however, lead to difficulties for a complete quantitative discussion of the XPS data. A comparison with the spectra of Cu exposed to the solvents without ODT (Fig. 4a) shows the absence of a carbide-like C fraction in the C 1s peak. The intensity ratios of the components of the C 1s peak are also obviously far from consistent with adsorption of ethanolate, as a 1:1 ratio of C-C/H and C-O species would be expected in that case. We reason therefore that adsorption or reaction of solvent species alone are is not the direct cause of the strong carbide-like C 1s signal observed here. Ethanolate adsorption may, however, contribute to the C-S bond weakening through interactions with the adsorbed thiol species.

The formation of Cu-C bonds would not necessarily be expected in such a system. Copper organyls are typically unstable in solution in air or the presence of moisture.[57] On the other hand, in interfacial systems, highly reactive species may be shielded; for example, the presence of highly reactive aluminium hydride has been shown by secondary ion mass spectrometry on aluminium exposed to aqueous solutions.[58] Recently, monolayers of N-heterocyclic carbenes on many metals have been prepared,[59] including copper.[60] Such systems show high stability, due to the steric shielding of the metal carbon bonds.[61] The analytical data obtained in this work suggests that a bonding situation similar to those systems develops at the metal/organic interface, where presumably the oxide or sulfide take the shielding role. It is worth noting that for N-heterocyclic carbene SAMs, the C 1s signal of the metal binding carbon has been reported as very close to the C 1s of aliphatic carbon from the remaining molecule.[62] However, as the vicinity of two electronegative N-atoms to

the metal-binding C would lead to the expectation of a higher binding energy than aliphatic carbon, one could reason that for these systems, the C 1s binding energy also shifts to lower values.

In this work, short-term stability has been assessed by LSV at pH 8.6 and 13.2. At pH 8.6, copper is passive, while pH 13.2 is in the region where the passivating CuO partly dissolves under cuprate formation.[63] The measured E_{corr} show that copper is not immune in the chosen electrolytes. Values of i_{corr} and R_{P} also show that passivity is better in borate buffer, as expected. Therefore, the discussion shall focus on the system in NaOH. Cathodic branches of the LSV experiments (Fig. 2) show that on oxide-covered copper, ORR can proceed, while the ORR is inhibited on the SAM-covered surfaces. Here, ORR may only occur at domain boundaries. Interestingly, this inhibition is much stronger for ODT from ethanol than for ODT from THF. In the ODT/ethanol sample, the ORR inhibition is so strong that the cathodic branch cannot be explained purely by a diffusion controlled process. The lower i_{corr} is likely in part related to the inhibition of the ORR. The anodic branches of the LSV experiment may be interpreted such that at potentials above E_{corr}, the surface passivated by Cu_2O formation. Above ≈70 mV, Cu_2O is oxidised to Cu^{II}, explaining the increase in current density after passivation set in. At higher potentials, CuO formation should inevitably set in, as the solution near the surface became saturated with Cu^{2+}. In line with previous studies,[21] the organic layer protects the surface in such short-term experiments, reflected in lower i_{corr} and higher R_{P}. The system that contained least oxide, prepared in ethanol, shows the lowest i_{corr} and highest R_{P}. Thus, despite the chemical reaction at the surface, ODT/ethanol samples show a well protected surface. The oxide-rich samples prepared from THF shows higher corrosion rates.

The trends observed in the contact angle experiments mirrors the trends discussed from LSV experiments. Samples modified in ODT show the lowest content of oxide, and thus the highest contact angle. The differences in initial contact angle also reflect the initial differences in structure between the differently prepared layers. The different behavior of the water

droplet with time is likely related to the stability of the sample surface. Initially, the organic molecules protect the metal surface, repelling the water droplet. With time, however, the water can penetrate through the organic molecules and approachs the metal/SAM interface, leading to degradation of the protective layer. Indeed, copper oxide reforms, under structural relaxation of the SAM, e.g. during exposure to the atmosphere.[24–27] In the THF samples, the initial amount of oxide is larger - leading to a lower contact angle initially, but also a contact angle which remains more constant with time.

Conclusions

In THF, ODT forms a classical SAM, however, oxide is present at the surface when prepared under ambient conditions. More interesting is the situation in ethanol. At an ODT-covered surface, the presence of Cu_2S and sulfur-carbon bonding indicates a decomposition of the thiol. Such a decomposition has not been observed in previous works on thiols on copper to the knowledge of these authors. The fact that the decomposition occurs only in ethanol implies that the solvation of the tiol in ethanol weakens the S-C bond in the thiolate. The resulting surfaces have a larger polarisation resistance and show lowest corrosion current densities from the systems investigated here. Both systems are stable during linear polarization experiments within a potential window of ± 150 mV around the initial corrosion potential. Both preparations show a protecting effect, supporting observations from literature. IR spectroscopy indicates crystalline close packing of chains in all trans conformation in the ODT monolayers prepared from both ethanol and THF. Oxide reduction is observed both in THF and ethanol, comparing the intensities of the respective O 1s peak in XPS. However, the amount of oxide is larger in THF compared to ethanol. Overall, formation of Cu-C bonds in this system opens up interesting opportunities for the preparation of SAMs beyond the metal-thiol bonding on reactive metals.

Acknowledgement

A.E. acknowledges Prof. M. Stratmann for continuous support. The authors thank E. Heinen for preparation of silicon wafers. M.K. acknowledges Rector's Habilitation Grant 14/ 990/ RGH18/ 0104.

References

(1) Gooding, J. J.; Mearns, F.; Yang, W.; Liu, J. Self-assembled monolayers into the 21st century: recent advances and applications. *Electroanalysis* **2003**, *15*, 81–96.

(2) Love, J. C.; Estroff, L. A.; Kriebel, J. K.; Nuzzo, R. G.; Whitesides, G. M. Self-assembled monolayers of thiolates on metals as a form of nanotechnology. *Chem. Rev.* **2005**, *105*, 1103–1170.

(3) Vericat, C.; Vela, M. E.; Benitez, G.; Carro, P.; Salvarezza, R. C. Self-assembled monolayers of thiols and dithiols on gold: new challenges for a well-known system. *Chem. Soc. Rev.* **2010**, *39*, 1805.

(4) Vericat, C.; Vela, M. E.; Corthey, G.; Pensa, E.; Cortés, E.; Fonticelli, M. H.; Ibanez, F.; Benitez, G.; Carro, P.; Salvarezza, R. C. Self-assembled monolayers of thiolates on metals: a review article on sulfur-metal chemistry and surface structures. *RSC Adv.* **2014**, *4*, 27730–27754.

(5) Käfer, D.; Witte, G.; Cyganik, P.; Terfort, A.; Wöll, C. A Comprehensive Study of Self-Assembled Monolayers of Anthracenethiol on Gold: Solvent Effects, Structure, and Stability. *J. Am. Chem. Soc.* **2006**, *128*, 1723–1732.

(6) Bensebaa, F.; Voicu, R.; Huron, L.; Ellis, T. H.; Kruus, E. Kinetics of Formation of Long-Chain n-Alkanethiolate Monolayers on Polycrystalline Gold. *Langmuir* **1997**, *13*, 5335–5340.

(7) Yamada, R.; Sakai, H.; Uosaki, K. Solvent Effect on the Structure of the Self-Assembled Monolayer of Alkanethiol. *Chem. Lett.* **1999**, *28*, 667–668.

(8) Shen, C.-H.; Lin, J.-C. Improving the Surface Biocompatibility with the Use of Mixed Zwitterionic Self-Assembled Monolayers Prepared by a Proper Solvent. *Langmuir* **2011**, *27*, 7091–7098.

(9) Lee, S. Y.; Choi, Y.; Ito, E.; Hara, M.; Lee, H.; Noh, J. Growth, solvent effects, and thermal desorption behavior of octylthiocyanate self-assembled monolayers on Au(111). *Phys. Chem. Chem. Phys.* **2013**, *15*, 3609–3617.

(10) Hamoudi, H.; Dablemont, C.; Esaulov, V. A. Disorder, solvent effects and substitutional self-assembly of alkane dithiols from alkane thiol SAMs. *Surf. Sci.* **2011**, *605*, 116 – 120.

(11) Umemura, K.; Fujita, K.; Ishida, T.; Hara, M.; Sasabe, H.; Knoll, W. Solvent Effect on Domain Formation of 4-Mercaptopyridine Self-Assembled Monolayers on Au(111) Substrate by Scanning Tunneling Microscopy. *Jap. J. Appl. Phys.* **1998**, *37*, 3620–3625.

(12) Mekhalif, Z.; Laffineur, F.; Couturier, N.; Delhalle, J. Elaboration of Self-Assembled Monolayers of n-Alkanethiols on Nickel Polycrystalline Substrates: Time, Concentration, and Solvent Effects. *Langmuir* **2003**, *19*, 637–645.

(13) Whelan, C. M.; Kinsella, M.; Ho, H. M.; Maex, K. Corrosion Inhibition by Thiol-Derived SAMs for Enhanced Wire Bonding on Cu Surfaces. *J. Electrochem. Soc.* **2004**, *151*, B33–B38.

(14) Ron, H.; Cohen, H.; Matlis, S.; Rappaport, M.; Rubinstein, I. Self-assembled monolayers on oxidized metals. 4. Superior n-alkanethiol monolayers on copper. *J. Phys. Chem. B* **1998**, *102*, 9861–9869.

(15) Sung, M. M.; Sung, K.; Kim, C. G.; Lee, S. S.; Kim, Y. Self-assembled monolayers of alkanethiols on oxidized copper surfaces. *J. Phys. Chem. B* **2000**, *104*, 2273–2277.

(16) Zhang, Y.; Zhou, J.; Zhang, X.; Hu, J.; Gao, H. Solvent polarity effect on quality of n-octadecanethiol self-assembled monolayers on copper and oxidized copper. *Appl. Surf. Sci.* **2014**, *320*, 200 – 206.

(17) Zhang, Y.; Zhou, J.; Han, X.; Zhang, X.; Hu, J. Kinetics behavior of long-chain n-alkanethiols adsorbed on copper surface. *Appl. Surf. Sci.* **2015**, *353*, 979 – 985.

(18) Denayer, J.; Delhalle, J.; Mekhalif, Z. Surface modification of copper with 2-dodecylpropane-1,3-dithiol: The key effect of the solvent. *Appl. Surf. Sci.* **2009**, *256*, 1426 – 1430.

(19) Fonder, G.; Laffineur, F.; Delhalle, J.; Mekhalif, Z. Alkanethiol-oxidized copper interface: the critical influence of concentration. *J. Colloid Interface Sci.* **2008**, *326*, 333–338.

(20) Gong, Y. S.; Lee, C.; Yang, C. K. Atomic force microscopy and Raman spectroscopy studies on the oxidation of Cu thin films. *J. Appl. Phys.* **1995**, *77*, 5422–5425.

(21) Laibinis, P. E.; Whitesides, G. M. Self-assembled monolayers of n-alkanethiolates on copper are barrier films that protect the metal against oxidation by air. *J. Am. Chem. Soc.* **1992**, *114*, 9022–9028.

(22) Keller, H.; Simak, P.; Schrepp, W.; Dembowski, J. Surface chemistry of thiols on copper: an efficient way of producing multilayers. *Thin Solid Films* **1994**, *244*, 799–805.

(23) Wallace, T. J. Reactions of Thiols with Metals. I. Low-Temperature Oxidation by Metal Oxides. *J. Org. Chem.* **1966**, *31*, 1217–1221.

(24) Hosseinpour, S.; Forslund, M.; Johnson, C. M.; Pan, J.; Leygraf, C. Atmospheric corrosion of Cu, Zn, and Cu-Zn alloys protected by self-assembled monolayers of alkanethiols. *Surf. Sci.* **2016**, *648*, 170 – 176.

(25) Hosseinpour, S.; Johnson, C. M.; Leygraf, C. Alkanethiols as Inhibitors for the Atmospheric Corrosion of Copper Induced by Formic Acid: Effect of Chain Length. *J. Electrochem. Soc.* **2013**, *160*, C270–C276.

(26) Schwind, M.; Hosseinpour, S.; Johnson, C. M.; Langhammer, C.; Zorić, I.; Leygraf, C.; Kasemo, B. Combined in Situ Quartz Crystal Microbalance with Dissipation Monitoring, Indirect Nanoplasmonic Sensing, and Vibrational Sum Frequency Spectroscopic Monitoring of Alkanethiol-Protected Copper Corrosion. *Langmuir* **2013**, *29*, 7151–7161.

(27) Hosseinpour, S.; Schwind, M.; Kasemo, B.; Leygraf, C.; Johnson, C. M. Integration of Quartz Crystal Microbalance with Vibrational Sum Frequency Spectroscopy–Quantification of the Initial Oxidation of Alkanethiol-Covered Copper. *J. Phys. Chem. C* **2012**, *116*, 24549–24557.

(28) Yarimbiyik, A. E.; Schafft, H. A.; Allen, R. A.; Vaudin, M. D.; Zaghloul, M. E. Experimental and simulation studies of resistivity in nanoscale copper films. *Microelectron. Reliab.* **2009**, *49*, 127 – 134.

(29) Blaudez, D.; Buffeteau, T.; Desbat, B.; Orrit, M.; Turlet, J. Characterization of Langmuir-Blodgett monolayers using polarization modulated FTIR spectroscopy. *Thin Solid Films* **1992**, *210-211*, 648 – 651.

(30) Erbe, A.; Sarfraz, A.; Toparli, C.; Schwenzfeier, K.; Niu, F. In *Soft Matter at Aqueous Interfaces, Lect. Notes Phys.*; Lang, P. R., Liu, Y., Eds.; Springer: Cham, Switzerland, 2016; Vol. 917; Chapter 14 - Optical Absorption Spectroscopy at Interfaces, pp 459–490.

(31) Crist, B. V. A review of XPS data-banks. *J. XPS Rep.* **2007**, *1*, 1–52.

(32) Kim, H.; Colavita, P. E.; Paoprasert, P.; Gopalan, P.; Kuech, T.; Hamers, R. J. Grafting of molecular layers to oxidized gallium nitride surfaces via phosphonic acid linkages. *Surf. Sci.* **2008**, *602*, 2382–2388.

(33) Deroubaix, G.; Marcus, P. X-ray photoelectron spectroscopy analysis of copper and zinc oxides and sulphides. *Surf. Interface Anal.* **1992**, *18*, 39–46.

(34) Powell, C. J.; Jablonski, A. Evaluation of calculated and measured electron inelastic mean free paths near solid surfaces. *J. Phys. Chem. Ref. Data* **1999**, *28*, 19–62.

(35) Friis, E. P.; Andersen, J. E.; Madsen, L. L.; Bonander, N.; Møller, P.; Ulstrup, J. Dynamics of Pseudomonas aeruginosa azurin and its Cys3Ser mutant at single-crystal gold surfaces investigated by cyclic voltammetry and atomic force microscopy. *Electrochim. Acta* **1998**, *43*, 1114–1122.

(36) Stern, M.; Geary, A. L. Electrochemical polarization I. A theoretical analysis of the shape of polarization curves. *J. Electrochem. Soc.* **1957**, *104*, 56–63.

(37) Snyder, R. G.; Strauss, H. L.; Elliger, C. A. Carbon-hydrogen stretching modes and the structure of n-alkyl chains. 1. Long, disordered chains. *J. Phys. Chem.* **1982**, *86*, 5145–5150.

(38) Macphail, R.; Strauss, H.; Snyder, R.; Elliger, C. C-H stretching modes and the structure of normal alkyl chains. 2. Long, all-trans chains. *J. Phys. Chem.* **1984**, *88*, 334–341.

(39) Nuzzo, R. G.; Dubois, L. H.; Allara, D. L. Fundamental studies of microscopic wetting on organic surfaces. 1. Formation and structural characterization of a self-consistent series of polyfunctional organic monolayers. *J. Am. Chem. Soc.* **1990**, *112*, 558–569.

(40) Kühnle, A.; Vollmer, S.; Linderoth, T. R.; Witte, G.; Besenbacher, F. Adsorption of Dodecanethiol on Cu(110): Structural Ordering upon Thiolate Formation. *Langmuir* **2002**, *18*, 5558–5565.

(41) Schmidt, C.; Götzen, J.; Witte, G. Temporal Evolution of Benzenethiolate SAMs on Cu(100). *Langmuir* **2011**, *27*, 1025–1032.

(42) Wang, Y.; Im, J.; Soares, J. W.; Steeves, D. M.; Whitten, J. E. Thiol Adsorption on and Reduction of Copper Oxide Particles and Surfaces. *Langmuir* **2016**, *32*, 3848–3857.

(43) Wagner, C.; Naumkin, A.; Kraut-Vass, A.; Allison, J.; Powell, C.; Rumble Jr, J. *NIST X-ray photoelectron spectroscopy database; NIST standard reference database 20, version 3.5 (Web version)*; National Institute of Standards and Technology: Gaithersburg, 2007.

(44) Pattrick, R. A. D.; Mosselmans, J. F. W.; Charnock, J. M.; England, K. E. R.; Helz, G. R.; Garner, C. D.; Vaughan, D. J. The structure of amorphous copper sulfide precipitates: An X-ray absorption study. *Geochim. Cosmochim. Acta* **1997**, *61*, 2023–2036.

(45) Buckley, A. N.; Woods, R. An X-ray photoelectron spectroscopic study of the oxidation of chalcopyrite. *Austral. J. Chem.* **1984**, *37*, 2403–2413.

(46) Powell, C.; Jablonski, A. *NIST Electron Inelastic-Mean-Free-Path Database, Version 1.2, SRD 71*; National Institute of Standards and Technology: Gaithersburg, 2010.

(47) Tanuma, S.; Powell, C. J.; Penn, D. R. Calculations of electron inelastic mean free paths. IX. Data for 41 elemental solids over the 50 eV to 30 keV range. *Surf. Interface Anal.* **2011**, *43*, 689–713.

(48) Krylova, V.; Andrulevičius, M. Optical, XPS and XRD studies of semiconducting copper sulfide layers on a polyamide film. *Int. J. Photoenergy* **2009**, *2009*.

(49) Watts, J.; Wolstenhome, J. *An introduction to surface analysis by XPS and AES*; Wiley: Chichester, 2003; pp. 8-10.

(50) Hurley, B. L.; McCreery, R. Covalent bonding of organic molecules to Cu and Al alloy 2024 T3 surfaces via diazonium ion reduction. *J. Electrochem. Soc.* **2004**, *151*, B252–B259.

(51) Heister, K.; Zharnikov, M.; Grunze, M.; Johansson, L.; Ulman, A. Characterization of X-ray induced damage in alkanethiolate monolayers by high-resolution photoelectron spectroscopy. *Langmuir* **2001**, *17*, 8–11.

(52) Ramírez, E. A.; Cortés, E.; Rubert, A. A.; Carro, P.; Benítez, G.; Vela, M. E.; Salvarezza, R. C. Complex Surface Chemistry of 4-Mercaptopyridine Self-Assembled Monolayers on Au(111). *Langmuir* **2012**, *28*, 6839–6847.

(53) Ossowski, J.; Wächter, T.; Silies, L.; Kind, M.; Noworolska, A.; Blobner, F.; Gnatek, D.; Rysz, J.; Bolte, M.; Feulner, P.; Terfort, A.; Cyganik, P.; Zharnikov, M. Thiolate versus Selenolate: Structure, Stability, and Charge Transfer Properties. *ACS Nano* **2015**, *9*, 4508–4526.

(54) Ossowski, J.; Nascimbeni, G.; Åżaba, T.; Verwüster, E.; Rysz, J.; Terfort, A.; Zharnikov, M.; Zojer, E.; Cyganik, P. Relative Thermal Stability of Thiolate- and Selenolate-Bonded Aromatic Monolayers on the Au(111) Substrate. *J. Phys. Chem. C* **2017**, *121*, 28031–28042.

(55) Ossowski, J.; Rysz, J.; Terfort, A.; Cyganik, P. Relative Stability of Thiolate and Selenolate SAMs on Ag(111) Substrate Studied by Static SIMS. Oscillation in Stability of Consecutive Chemical Bonds. *J. Phys. Chem. C* **2017**, *121*, 459–470.

(56) Mali, K. S.; Lava, K.; Binnemans, K.; De Feyter, S. Hydrogen Bonding Versus van der Waals Interactions: Competitive Influence of Noncovalent Interactions on 2D Self-Assembly at the Liquid-Solid Interface. *Chem. - Eur. J.* **2010**, *16*, 14447–14458.

(57) Wiberg, N. *Hollemann-Wiberg - Lehrbuch der Anorganischen Chemie, 101st edition*; Walter de Gruyter: Berlin, 1995; p. 1331-1332.

(58) Adhikari, S.; Lee, J.; Hebert, K. R. Formation of Aluminum Hydride during Alkaline Dissolution of Aluminum. *J. Electrochem. Soc.* **2008**, *155*, C16–C21.

(59) Engel, S.; Fritz, E.-C.; Ravoo, B. J. New trends in the functionalization of metallic gold: from organosulfur ligands to N-heterocyclic carbenes. *Chem. Soc. Rev.* **2017**, *46*, 2057–2075.

(60) Larrea, C. R.; Baddeley, C. J.; Narouz, M. R.; Mosey, N. J.; Horton, J. H.; Crudden, C. M. N-Heterocyclic Carbene Self-assembled Monolayers on Copper and Gold: Dramatic Effect of Wingtip Groups on Binding, Orientation and Assembly. *ChemPhysChem* **2017**, *18*, 3536–3539.

(61) Adhikari, B.; Meng, S.; Fyta, M. Carbene-mediated self-assembly of diamondoids on metal surfaces. *Nanoscale* **2016**, *8*, 8966–8975.

(62) Jiang, L.; Zhang, B.; Médard, G.; Seitsonen, A. P.; Haag, F.; Allegretti, F.; Reichert, J.; Kuster, B.; Barth, J. V.; Papageorgiou, A. C. N-Heterocyclic carbenes on close-packed coinage metal surfaces: bis-carbene metal adatom bonding scheme of monolayer films on Au, Ag and Cu. *Chem. Sci.* **2017**, *8*, 8301–8308.

(63) De Zoubov, N.; Vanleugenhaghe, C.; Pourbaix, M. In *Atlas of electrochemical equilibria in aqueous solutions*; Pourbaix, M., Ed.; National Association of Corrosion Engineers / Centre Belge d'Etude de la Corrosion CEBELCOR: Houston / Bruxelles, 1974; Chapter 14.1 - Copper, pp 384–392.

Graphical TOC Entry